LETTERS IN BIOMATHEMATICS
An International Journal

RESEARCH ARTICLE

OPEN ACCESS

A Spatiotemporal Network Modeling of Gut Microbiome Response to Targeted Nano-Drug Therapeutics in Human Gastrointestinal Systems

Tahniat Rehman[1*]

[1] Department of Nutrition and Dietetics, The University of Faisalabad, Pakistan

ABSTRACT

With the goal to comprehend the biological responses of bacteria exposed to nano-drugs in a spatiotemporally organized biological system, this work presents a mathematical model that was developed quantitatively. Non-linear population dynamics, migration, spatiotemporal drug transport and degradation, and regulation based on treatment outcome are all considered in the formulation. This study investigates trajectory analysis, network analysis, equilibrium, and stability of parameters, in contrast to previous approaches that just assess the impact of therapy based on concentration data. The non-dimensional form is used to identify dominating factors influencing system evolution and to assess the conflict between biological and transport phenomena on the same scale. While the spatial method shows the variety in drug concentration and distribution, numerical trajectories show bounded population behaviors and changes in the community's structure throughout treatment. Stability analysis may be used to discover parameter areas that correlate to robust and stable communities, while sensitivity analysis can be used to establish which parameters have the biggest impact on treatment results. Therapy regimens may be compared from several angles using a composite indicator of therapeutic response. In order to analyze microbial composition, exposure, and dynamic stability, this work's most significant novelty is the integration of the dynamic character of ecology with spatial drug transport and network factors inside a single mathematical modeling framework. A mechanistically based model for treatment-induced community changes has been made possible by the findings.

ARTICLE HISTORY
Received March 25, 2025
Accepted December 23, 2025

KEYWORDS
Nano-drug Transport,
Spatial Microbial Ecology,
Generalized Lotka-Volterra Model,
Interaction Networks,
Stability Analysis,
Dynamic Stability

1. Introduction

The relationship between human health and nutrition has increasingly attracted the attention of numerous researchers over recent years. The foods we consume influence our bodies in various ways, including immune function, energy levels, and disease risk. However, the specific mechanisms through which food impacts our bodily systems remain inadequately understood (Li et al., 2024). For numerous years, researchers have been studying it and have uncovered different theories and findings that enhance our understanding of the relationship between diet and human health. A particularly important factor in this context is the gut microbiome (Culp & Goodman, 2023). The progress in metagenomics, metabolomics, and systems biology has demonstrated that the gut microbiome functions as a complex ecological network, with its architecture continually altering in response to environmental stresses, dietary consumption, illness states, and drugs. However, despite the quick collection of biological data utilizing improved technologies, the interpretation of these findings remains difficult (Luo et al., 2024).

However, because of the temporal and geographical variability along the human gut caused by a dynamic interaction between the host, microbes, and environment, this is still difficult (Geng et al., 2021). According to biomathematics, the gut microbiome is a complex adaptive system made up of a community of interacting

CONTACT Tahniat Rehman:tahniatrehman.DND@tuf.edu.pk

microbial species linked by competitive and collaborative interactions, metabolites exchange, and host organism control. Mathematical models allow us to measure the dynamics of microbial populations, evaluate the intensity of connections, identify network hubs, and forecast community behavior in the face of external disturbances (Lange et al., 2024). Notably, network analysis approaches have proven to be highly successful in the study of large-scale microbiome datasets (Luo et al., 2024).

The formation of infection is significantly influenced by stochastic effects resulting from spatial factors, such as the local availability of target and immune cells, which can result in various infection outcomes (Sego et al., 2020). For instance, models that characterize microbial-microbial interactions without taking time dependency into account include similarity-based and rule-mining (Zhang et al., 2018). Many classical compartmental models overlook these spatial characteristics, resulting in model predictions that are less accurate for use in biological systems. Recent research has focused on the need for spatiotemporal modeling tools that can help capture microorganisms' mobility, diffusion processes, colonization, and localized treatment reactions (Urtecho et al., 2024). The physicochemical properties of nano-drug carriers allow for increased bioavailability, regulated drug delivery, targeted localization, and efficacy. According to recent studies, nanotherapies interact with gut bacteria to alter the organization of the microbiota population in addition to affecting host tissues (Garbati et al., 2024).

In order to describe these mechanisms quantitatively, the microbiome must be viewed as a coupled nonlinear dynamic system in which network dynamics, population dynamics, and spatial movement all occur simultaneously (Simonson et al., 2025). Because it links modified Lotka-Volterra equations for microbial population dynamics with reaction diffusion advection equations and the adaptive interaction network, the suggested theoretical framework mathematically expands on earlier models of the microbiome. We can examine the trajectories, gradients, equilibria, and network changes in the same state space using such a model framework. In order to examine the response and perturbation effects, we thus consider the application of therapeutic treatment as a dynamic forcing function, not only the concentration. Additional quantitative indications of system behavior include normalized sensitivity coefficients, topological features of the network, and Jacobian-based stability analysis. Additionally, the multidimensional therapeutic response can be reduced to a numerically analyzable number using the Therapeutic Response Index (TRI). As a result, this framework integrates network theory, spatial processes, and nonlinear dynamics into a single biomathematical model.

2. Research Objective of Study

The purpose of this study is to examine the effects of non-linear population interaction, migration, drug dispersion in space, drug degradation, and microbial effects. In order to offer a quantitative analysis of the microbial response to treatments and the mechanisms causing it, particular attention will be paid to changes in the community structure, stability, spatial distribution, and sensitivity of factors.

3. Literature Review

Several studies have shown that the effects of a person's food on the immune system, gut microbiota, and other bodily systems and the connections between these systems have also been thoroughly explained in this study piece. Many researchers have looked into the many biological mechanisms and pathways to explain how these systems have affected the sickness and general health of the body, rather than only looking at broad correlations between them (Gupta et al., 2025). Study focused on the function of microorganisms, and it was emphasized that the microbiome functions as a biochemical factory that is useful in generating substances that have a direct impact on host pathway signaling and microbial metabolites affect hormone synthesis, glucose metabolism, and hunger control (Alzubadi, 2025). Scholars have extensively used computational and mathematical modeling tools to understand complex biological processes. It was discovered that these advanced computational and mathematical models assist researchers in predicting interactions between microorganisms and immune system (Hadjigeorgiou et al., 2025). According to Luo et al. (2024), the network biology framework is an effective tool for connecting the mechanistic and machine learning approaches because it preserves interaction linkages while allowing for comprehensive data integration. This study underlined the significance of network topology as a strategy for identifying major microbe regulators and organizational patterns in microbial communities. Research shows that Gonzalez-Garcia et al. (2025) developed mechanistic microbiome models clearly incorporate biological assumptions, resulting in greater interpretability and prediction than statistical modeling alone. These models have proven particularly beneficial in studying host-microbiome interactions and ecological stability. It has been established that graph-theoretic representations of the dataset outperform feature-based algorithms at capturing highly connected microbiome data. This underlines the importance of network science in microbiome investigation and highlights the need to

incorporate graph dynamics into the therapeutic modeling framework (Irwin et al., 2024). Experimental studies have revealed that the distribution of microbial communities along the gastrointestinal tract is non-uniform, and that ecological niches exist, resulting in the development of region-specific communities. According to Urtecho et al. (2024), the process of colonization by microbial communities exhibits considerable spatiotemporal dynamics that cannot be represented using non-spatial models. Nano-drug transport systems have been shown to increase drug targeting efficiency, improve control over drug release, and reduce toxicity (Garbati et al., 2024). Some experiments have shown that nanomaterials can have a considerable impact on microbial communities and their metabolic activity, the majority of current research on the topic is descriptive rather than quantitative. Recent research has highlighted the significance of microbial interaction networks in regulating inflammation, metabolism, and therapeutic response. The communication between bacteria, metabolic cooperativity, and competitive exclusion are all significant factors in determining ecosystem resilience and response to drugs (Lawing & Bleich, 2025). According to research, existing models continue to be inadequate since they are limited to studying microbial interaction networks, temporal characteristics, spatial disparities, and treatments separately (Sieders et al., 2025). The relationships can be described using statistical and machine learning-based approaches, but they offer very little mechanistic insight into nonlinear feedbacks, parameter dependencies, equilibria, and dynamical stability. Similarly, certain transport models cannot take the produced exposure field into account when adjusting microbial interaction coefficients. Therefore, when population dynamics, transport, adaptive network dynamics, and treatment forces interact in a system, there is a mathematical gap in the formulation of the coupled dynamics. By combining all of the previously described mathematical components into a unified spatiotemporal framework for evaluating the impact of treatments on gut microbiota dynamics, the current study seeks to close this gap.

4. Research Methodology

The suggested model is expressed in terms of a nonlinear dynamical coupled system with theoretically well-defined state constraints and biologically plausible assumptions. The generalized Lotka-Volterra coefficients have been used to represent the microbial interactions, and a one-dimensional heterogeneous domain has been used to account for the spatial variation. The reaction-diffusion-advection process of nano-drug transport allows for the independent consideration of diffusion, directed motion, degradation, and release as contributing factors in the system dynamics. The model takes into account that the concentration of pharmaceuticals and bacteria is non-negative, and that the carrying capacities and interaction rates for controlling the growth rate of microbes vary gradually.

4.1. Formulation of Model

Consider meta-community dynamics in the simplest chain network, which consists of two patches: an upstream and a downstream patch. If an upstream species k consumes a resource that a downstream species i needs, it will have a negative influence on the downstream species growth (negative a_{ik}). Beneficial byproducts produced by species k in the upstream community have a favorable effect on the growth of species i in the downstream patch (positive a_{ik}). A generalized Lotka-Volterra (gLV) model was used to explain the dynamics of species $i's$ abundance ($i = 1, \ldots, N$) in patch j, where $j = 1,2$ denotes up- and downstream patches, respectively.

$$\frac{dx_{i1}}{dt} = x_{i1}(r_{i1} + \sum_{k=1}^{N} a_{ik}x_{k1}) \quad (1)$$

$$\frac{dx_{i2}}{dt} = x_{i2}(r_{i2} + \sum_{k=1}^{N} a_{ik}(x_{k1} + x_{k2}) \quad (2)$$

where N is the maximum number of species in a patch, represents species $i's$ abundance in patch j, is the intrinsic growth rate of species i in patch j, and a_{ik} represents the net interaction from species k to i. Although gLV models reflect species interactions phenomenological, we assume that all species interact indirectly, such as secreting or absorbing chemical substances that are not explicitly specified in the model. To simplify, we scaled the interaction parameters so that $a_{ii} = -1$ for all i. This ensures that the abundance of species i in patch j is $x_{ij}^{*} = r_{ij}$ at equilibrium in monoculture. This formulation just contains the patches upstream and downstream. The gut's governing equation becomes

$$\frac{\partial M_i}{\partial t} = f_i(M) + D_i\nabla^2 M_i + T_i(M, N) \quad (3)$$

The gastrointestinal system has a high degree of heterogeneity due to changes in pH, nutrition, oxygen concentration, mucin content, and host immunity. As a result of this heterogeneity, microorganisms are unevenly distributed along the digestive axis. To reflect biological reality, the gut system is represented as a spatially

distributed system in which the microbial population varies across time and space.

4.1.1. Generalized Lotka-Volterra Model

This model is represented by the following equation:

$$\frac{dn_i(t)}{dt} = \frac{r_i}{k_i} n_i(t)\left[k_i - n_i(t) - \sum_{j\epsilon\partial i} \alpha_{ij} n_j(t)\right] + \xi_i(t) \quad (4)$$

$n_i(t)$ indicates the abundance of species at time t, while ∂i represents the set of species that interact with species i. We will focus on random graphs where the cardinality of ∂i is fixed and equal to $k_i = 3$ for all $i's$. However, the approaches we utilize can be applied with no modification to a Poissonian distribution of the connectivities $k_i's$. The factors r_i and k_i are respectively the intrinsic growth rate and carrying capacity of species i, while $\xi_i(t)$ represents a Gaussian multiplicative noise with zero mean and covariance.

$$\langle \xi_i(t)\xi_i(t\hat{}) \rangle = 2Tn_i(t)\delta_{ij}\delta(t - t\hat{}) \quad (5)$$

By enhancing Lotka-Volterra model for nano-drug therapeutics, the equation becomes

$$\frac{\partial N}{\partial t} = D_N \nabla^2 - v\frac{\partial N}{\partial x} - \lambda N \quad (6)$$

In addition to microbial dissemination, therapeutic nanocarriers move spatially by diffusion, intestinal advection, and metabolic breakdown. The latter parameters influence the spatial concentration of drugs and thus play an essential role in the response of microbiomes in various locations.

4.2. Random Graphical Model

In this, random graphical model for network inference from diverse microbiome data from various locations is defined. Let $Y^{(k)}$ be the random vector of interest, that is abundance of p in environment k. We supposed $Y^{(k)}$ is distributed using a graphical model (GM).

$$Y^{(k)}|G^{(k)} \sim L_{G^{(k)}}(\Omega^{(k)}) \quad (7)$$

Relative to a conditional independence graph $G^{(k)}$ and related parameters $\Omega^{(k)}$. The graphs $G^{(k)}$ are dispersed using a joint random graph model.

$$G^{(k)} \sim P(\theta), \quad k = 1, \dots, B \quad (8)$$

The appropriate graphical or random graph model is determined by the circumstances at hand. Gaussian copula graphical model was chosen because of its simple mathematical formulation. This methodology is adaptable to non-Gaussian multivariate data, such as microbiome counts. Therefore, comparable to , we assumed:

$$P(Y_1^{(k)} \le y_1, \dots, Y_p^{(k)} \le y_p | G^{(k)}, \Omega^{(k)} = \emptyset_p(\emptyset^{-1}(F_1(y_1)), \dots, \emptyset^{-1}(F_1(y_1)); R^{(k)}) \quad (9)$$

In this equation (9), $\emptyset_p$ represents the cumulative distribution function of a p-dimensional multivariate normal with a zero mean vector and correlation matrix $R^{(k)} = \Omega^{(k)-1}$. $\emptyset$ is the usual univariate normal distribution function, and F_j is the marginal distribution of Operating Taxonomic Units (OTU) j. The conditional independence graph $G^{(k)}$) represents the model's induced dependency structure in condition k.

To account for the diversity of microbiome data, the marginal distribution of OUT j may be connected to external variables like body site and sequencing depth. To formalize this with the use of a parametric marginal model,

$$F_j(y_j|x) = 1 = q_j(x)^{(y_j+1)^{b_j(\infty)}} \quad (10)$$

$$\log\left(\frac{q_j(x)}{1-q_j(x)}\right) = x^t\eta_j, \ \log\left(b_j(x)\right) = x^t\gamma_j \quad (11)$$

The node covariates $x = (1, x_1, \dots, x_m)^T$ and regression coefficients η_j and γ_j correspond to the parameters of the discontinuous Weibull distribution, respectively. The copula's mapping to the latent Gaussian space (z_j = $\emptyset^{-1}$ (F_j (y_j)) is not unique due to the discontinuous nature of the data. Each observation (y_j, x) corresponds to an interval in the latent space, as shown by

$$I_{F_j}(y_j|x) = (\emptyset^{-1}\left(F_j(y_j - 1|x)\right), \emptyset^{-1}(F_j(y_j|x)) \quad (12)$$

4.3. Spatiotemporal Nan-Drug Transport Dynamics

Understanding the geographical and temporal distribution of the nano-drug therapeutic agent is necessary for studying the effect of targeted nano-drug therapy on the gut microbial community. The gastrointestinal system is naturally heterogeneous due to the presence of several ecological regions with varying physical and chemical characteristics. As a result, diffusion, advection from the movement of digestive fluids, degradation, and release of the nano-drug particle occur. Let $N\ (x,t)$ represent the concentration of nano-drugs at a given site x and time t. The transport phenomenon may be described using a reaction diffusion convection equation.

$$\frac{\partial N}{\partial t} = D_N \nabla^2 N - v\frac{\partial N}{\partial x} - \lambda N + R(x,t) \tag{13}$$

where, D_N represents the nano-drug diffusion coefficient, v denotes intestinal flow velocity, λ is showing drug degradation rate and $R(x,t)$ represents the controlled-release function. The release kinetics of nano-drug can be represented as

$$R(x,t) = kN_0 e^{-kt} \tag{14}$$

Where N_0 is the starting drug concentration, while k is the release constant. To determine biological validity, the total drug mass in the gastrointestinal tract can be quantified as follows:

$$M_N(t) = \int_{\Omega}^{1} N(x,t)dx \tag{15}$$

Ω represents the spatial domain of gut. This is a measure of therapeutic exposure that can be used to evaluate medication accumulation and clearance in a specific location. The integration of diffusion and transportation processes into the model provides a tool for predicting microbiome treatment responses. The average nano-drug concentration across the gastrointestinal domain can be described as

$$\overline{N}(t) = \frac{1}{|\Omega|}\int_{\Omega}^{1} N(x,t)dx \tag{16}$$

4.4. Coupled Spatiotemporal Microbiome Dynamics

The gut microbiome is modeled as a network of interacting microbial populations that spread throughout the digestive tract. A spatially explicit model formulation is required due to the variety of microbial growth and interaction processes throughout the intestines. As a result, the traditional Lotka-Volterra model is updated to incorporate diffusion and drug-induced effects. Let $(M_i(x,t))$ denote the abundance of microbial species. The dynamics are governed by

$$\frac{\partial M_i(x,t)}{\partial t} = D_i \nabla^2 M_i(x,t) + r_i M_i(x,t)\left(1 - \frac{M_i(x,t)}{K_i}\right) + M_i(x,t)\sum_{j=1}^{n} a_{ij} M_j(x,t) - \beta_i N(x,t)\, M_i(x,t) \tag{17}$$

Some of the mathematical characteristics required for biological relevance are present in the coupled model under study. The state variables take values from the positive orthant since microorganisms and drug concentrations are physical factors. The comparison principle can be used to determine that solutions will remain non-negative for all future times given non-negative initial data and positive diffusion and response terms.

Furthermore, the physiologically plausible region has locally Lipschitz continuous nonlinear functions related to growth and decay. Consequently, the system of coupled reaction-diffusion equations has a unique local solution according to Picard-Lindelöf's existence theorem. Drug degradation guarantees that the concentration of the pharmaceuticals cannot increase indefinitely, and the carrying capacity limits the proliferation of microorganisms. The region consequently turns into a positively invariant set.

By putting the temporal derivatives to zero, the equilibria may be calculated, resulting in steady-state medication concentrations and microbial levels. The eigenvalues of the Jacobian matrix can be used to examine the local asymptotic stability. When all of the eigenvalues' real parts are negative, the equilibrium is locally asymptotically stable. These characteristics define the model's state space, offering a mathematical basis for sensitivity analysis, network evolution, numerical simulation, and the interpretation of treatment-related perturbations. Therefore, rather than using numerical solutions, the model links the kinetics of an ecosystem with qualitative dynamic aspects. Diffusion reflects microbial migration from one neighboring site to another, whereas the interaction factor shows microbial cooperation and rivalry. The last element impacts the drug's effect on the microbe's development. Total Microbial Biomass is given by

$$B(t) = \sum_{i=1}^{n}\int_{\Omega}^{1} N(x,t)dx \tag{18}$$

The relative abundance of microbial specie i can be represented aa

$$P_i(t) = \frac{M_i(t)}{\sum_{j=1}^{n} M_j(t)} \tag{19}$$

The community diversity index can be expressed as

$$H(t) = \sum_{i=1}^{n} P_i(t) \ln P_i(t) \tag{20}$$

Monitoring $(B(t))$ helps in evaluating any change in the productivity of the ecosystem due to treatment. Coupling of microbial behavior and nano-drug transport is a great step compared to traditional ecosystem models which lack treatment.

4.5. Dynamic Microbial Interaction Network

Microbial populations are represented using network theory, which is continually changing in response to environmental and therapeutic pressures. In this scenario, the microbial species serve as network nodes, with edges representing ecological interactions between bacteria. The network is defined as

$$G(t) = \big(V, E(t)\big), \quad A(t) = \Big(a_{ij}(t)\Big) \tag{21}$$

$$\frac{da_{ij}}{dt} = \eta M_i M_j \tag{22}$$

Under this model, interactions strengthen when species interact frequently and weaken when drug is used. Overall network connection is assessed using

$$\emptyset(t) = \sum_{i=1}^{n} \sum_{j=1}^{n} a_{ij}(t) \tag{23}$$

The average interaction strength and network perturbation due to treatment can be defined as

$$\bar{A}(t) = \frac{1}{n(n-1)} \sum_{i \neq j} a_{ij}(t) \tag{24}$$

$$\Delta A(t) = A(t) - A(0) \tag{25}$$

This is used to determine the level of complexity in an ecosystem. The changes in demonstrate the impact of nanodrug on microbial communication routes.

4.6. Network Topological Analysis

Network topology provides information on the organization of microbial communities and aids in the identification of key regulators. The topological measurements are derived using the adjacency matrix, which is constantly changing. Degree centrality and between centrality can be computed as:

$$C_D(i) = \sum_{j=1}^{n} a_{ij}, \quad C_B(i) = \sum_{s \neq i \neq t}^{n} \frac{\sigma_{st}(i)}{\sigma_{st}} \tag{26}$$

The clustering coefficient and network density can be represented as

$$C_i = \frac{2e_i}{k_i(k_i-1)}, \quad \rho = \frac{2|E|}{n(n-1)} \tag{27}$$

$|E|$ denotes the number of edges. These quantifiable measures allow us to identify microbial hubs, highly linked species, and even treatment targets that promote ecosystem stability. The network modularity becomes:

$$Q = \frac{1}{2m} \sum_{ij} \left(a_{ij} - \frac{k_i k_j}{2m}\right) \delta(c_i, c_j) \tag{28}$$

4.7. Stability and Equilibrium Analysis

The mathematical analysis of equilibrium states is critical for understanding the microbiome's long-term dynamics following treatment. Equilibrium points can be discovered by setting the temporal derivatives equal to zero. The steady state equilibrium can be defined by

$$\frac{\partial M_i}{\partial t} = 0 \tag{29}$$

Thus,

$$\frac{\partial M_i}{\partial t} = D_i \nabla^2 M_i + r_i M_i \left(1 - \frac{M_i}{K_i}\right) + M_i \sum_{j=1}^{n} a_{ij} M_j - \beta_i N M_i = 0 \tag{30}$$

The jacobian matrix is

$$J = \left[\frac{\partial f_i}{\partial M_i}\right] \tag{31}$$

The equilibrium is locally asymptomatically stable if $Re(\lambda_k) < 0$ for all eigen values of λ_k of J. This study assesses microbial resilience to treatment perturbations.

4.8. Therapeutic Response Index

The Therapeutic Response Index (TRI) is offered as a quantitative measure of treatment success. The index compares the weighted microbial composition during treatment to the original microbial composition.

$$TRI(t) = \frac{\sum_{i=1}^{n} w_i M_i(t)}{\sum_{i=1}^{n} w_i M_i(0)} \tag{32}$$

The Therapeutic Response Index (TRI) is offered as a quantitative measure of treatment success.

$$\overline{TRI} = \frac{1}{T}\int_0^T TRI(t)dt \tag{33}$$

This provides a physiologically meaningful indication of microbiota recovery and therapeutic efficacy via targeted nanodrug administration.

4.9. Global Sensitivity Analysis

Sensitivity analysis is used to determine the significance of various model parameters and to identify biological pathways that have the greatest impact on treatment outcomes. The normalized sensitivity coefficient is computed as:

$$S_p = \frac{p}{Y}\frac{\partial Y}{\partial p} \tag{34}$$

Factors that have been investigated include microbial growth rate, carrying capacity, diffusion coefficient, interaction parameter, and antibiotic efficacy coefficient. Sensitivity parameters can be organized in the following order of importance:

$$S_{Ti} = 1 - \frac{Var(E[Y|p-i])}{Var(Y)} \tag{35}$$

Parameters with high absolute sensitivity have the greatest impact on system dynamics and so are excellent candidates for therapeutic optimization.

4.10. Model Parameters and Biological Interpretation

The biological, transport, and network characteristics that describe microbial development, ecological processes, transit, and treatment are part of the suggested biomathematical framework. The primary model parameters used in this work are listed in Table 1 along with their units, biological significance, and mathematical notation. For the connected spatiotemporal model system, table is a single point of reference.

Table 1: The Suggested Linked Spatiotemporal Network Model's Related Units, Mathematical Symbols, Model Parameters, and Biological Interpretations

Parameters	Description	Units	Biological Interpretation
$X_i(x,t)$	Abundance of microbial species i	CFUcm^{-1}	Population density of microbial species
$C(x,t)$	Nano-drug concentration	mgcm^{-3}	Spatial concentration of therapeutic agent
r_i	Intrinsic growth rate	day^{-1}	Natural microbial growth rate
K_i	Carrying capacity	CFUcm^{-1}	Maximum sustainable microbial population
a_{ij}	Interaction coefficient	Dimensionless	Competition or cooperation between species
D_m	Microbial diffusion coefficient	cm^2/day	Microbial spatial migration
D_d	Nano-drug diffusion coefficient	cm^2/day	Drug diffusion through gastrointestinal tissue
v	Advection velocity	cm/day	Intestinal flow velocity
λ	Drug degradation rate	day^{-1}	Nan-drug metabolic degradation
$R(t)$	Drug release function	mg/day	Controlled-drug release profile
γ_i	Drug sensitivity coefficient	Dimensionless	Species-species response to nano-drug
μ	Migration rate	day^{-1}	Microbial movement between gut regions
ρ	Migration allocation parameter	Dimensionless	Fraction migrating to upstream or downstream regions
TRI	Therapeutic Response Index	Dimensionless	Overall microbiome recovery measure

5. Results

5.1. Integrated Mathematical Framework for Nano-Drug Microbiome Interactions

Figure 1 shows the architectural structure of the spatiotemporal network model developed for studying the effects of nano-drug therapeutics on the gut microbial ecosystem. The first step of the framework starts with the representation of the gut as a heterogeneous spatial environment that comprises various ecological compartments due to variation in pH, nutrients, oxygen levels, mucins, and host immunity. This variation in environmental gradients creates spatial variations in microbial communities, thereby requiring spatial mathematical models.

The second step of the framework represents the transport dynamics of nano-drug therapy using a reaction-diffusion-advection system. These processes produce temporal concentration dynamics of the drug in the gut. The third component is the introduction of microbial population dynamics using a coupled reaction-diffusion generalized Lotka-Volterra model. The resulting microbial populations are then used to create dynamic interaction networks in which microbial taxa are represented as nodes and ecological interactions as weighted edges. This fourth section is on the adaptive evolution of microbial interaction networks under nano-drug pressure. This is the reorganization of the network as a result of changes in interaction weights. The final section of the biomathematical framework measures therapeutic outcomes using mathematical metrics such as the Therapeutic Response Index (TRI), topological indices, stability analysis, and global sensitivity analysis.

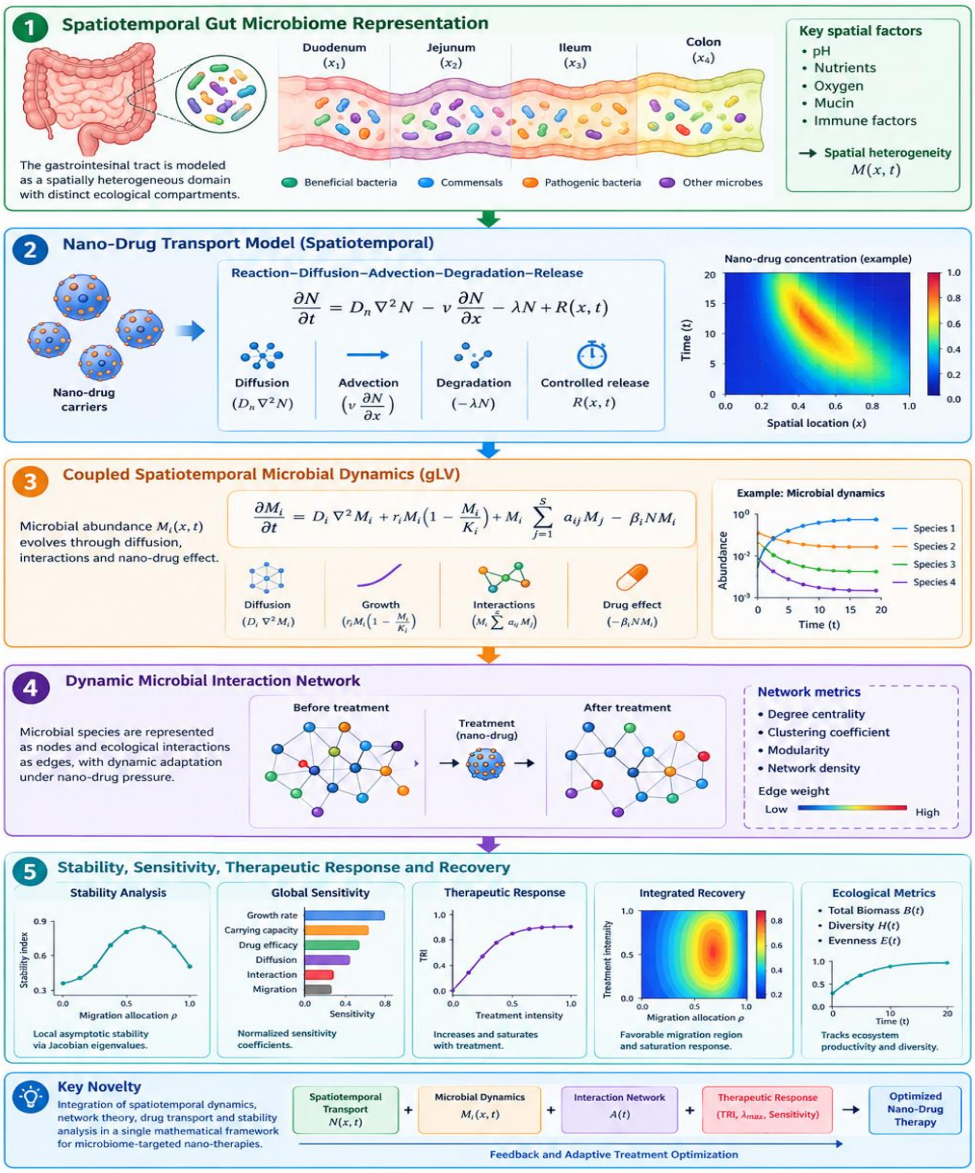


Figure 1: An Integrated Spatiotemporal Network Framework for Modeling Nano-Drug-Microbiome

5.2. Model-Derived Microbial Dynamics under Two-Patch Formulations

Table 2 displays the two-patch simulation's numerical state values. They are produced by the mathematical system and are not based on the real outcomes of any human measurements. Time instances are selected at random so that the trend and convergence of the microbes' redistribution can be seen without really looking at the Figure 2.

Table 2: Numerical Values used for Two-Patch Simulation

Time (day)	Upstream abundance	Downstream abundance
0.0	0.88	0.645
5.0	0.546	0.43
10.0	0.738	0.472
15.0	0.617	0.507
20.0	0.656	0.455
25.0	0.627	0.496
30.0	0.652	0.472

Figure 2 shows that bounded growth, interaction, and migration components have led to the evolution of the upstream and downstream states that were started in the positive orthant. Before reaching a positive asymptotic regime, the solution trajectories show damped nonlinear oscillations while staying bounded in the positive state space. According to the delayed redistribution through migration component, the downstream state reacted more slowly than the upstream state. Bounded phase trajectories stop unbounded population expansion and entail dynamical acceptability of the selected parameter space. From the perspective of the dynamical system, the equilibrium tendency illustrates how migration and interaction parameters work to regulate the asymptotic condition. The behavior that the defined dynamical system produces is more important than an observed population size.

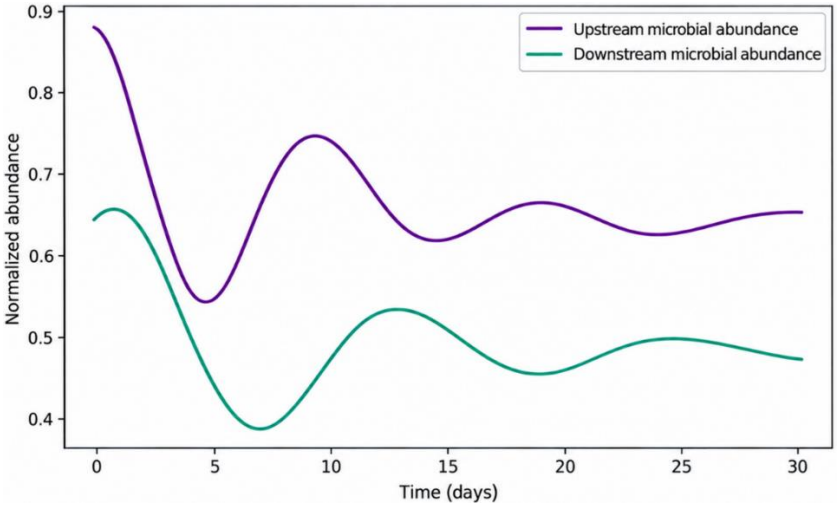


Figure 2: Upstream and Downstream Microbial Communities' Microbial Abundance Trajectories Using Model-Based Estimations Utilizing the Generalized Lotka-Volterra Equation of Two Patches

5.3. Specific Network Connection and Interaction Structure

Table 3 displays the primary network parameters that were calculated using the model's graphical states. While local triadic organization is shown by the clustering coefficient, network density is defined as the ratio of real edges. It is possible to depict treatment-related changes in connection as a mathematical network transition by mentioning both parameters.

Table 3: Primary Metrics for Network of Graphical States of the Model

Time Step	Network Density	Clustering Coefficient
0	0.18	0.11
1	0.23	0.15
2	0.29	0.19
3	0.34	0.24
4	0.3	0.21

5	0.26	0.17

In the Figure 3, it can be seen that the network's density increased in the start of the adaptive phase before falling to a reasonable level, but the clustering coefficient exhibited a pattern that was comparable to density but more gradual. As the group reacts to the pressure of therapy, this illustrates the brief increase in local organization followed by the network's relaxation. A drop in density suggests a partial decoupling or loss of weak ties, whereas an increase in density implies a growing number of pairwise relationships that become dynamically meaningful during the transition process. Before reaching a new network configuration, ecological neighborhoods tend to become more ordered, according to a clustering reaction.

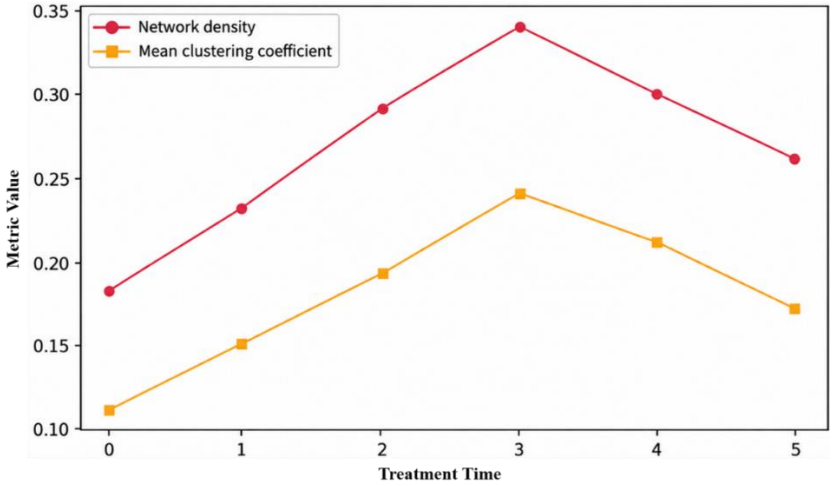


Figure 3: Changes in Mean Clustering and Density During Treatment-Induced Network Adaptation

5.4. Spatiotemporal Nano-Drug Transport and Exposure Gradients

Table 4 shows the numerical results from the response advection transport sub-model for particular time instants. While the drop in concentration is caused by degradation, the increase in dispersion is caused by diffusion, and the downstream displacement is associated with the advection process. To guaranty the independence of transport modeling, it is crucial to report each of these variables separately.

Table 4: Numerical Outputs of Reaction-Diffusion-Advection Transport at Different Time Points

Time (day)	Peak Position	Peak Concentration	Spatial Spread
0.0	0.20	0.92	0.08
4.0	0.35	0.76	0.12
8.0	0.50	0.61	0.16
12.0	0.64	0.48	0.20
16.0	0.77	0.37	0.24
20.0	0.88	0.29	0.27

The time-dependent nano-drug concentration pattern varied systematically over the gastrointestinal coordinate scale was found using the reaction-diffusion-advection model. The concentration maximum traveled along increasing spatial coordinates with increasing time, as seen in Figure 4, illustrating the advection effect. In the meantime, the diffusion effect was visible as the concentration pattern expanded in space. From a mathematical standpoint, the transport solution becomes a time-dependent spatial field whose peak is modified and its concentration distribution widens and weakens. Furthermore, the loss accumulated during the propagation phase is reflected in the decrease of the maximum. This output demonstrates that the scalar value of the treatment level alone does not determine the local level of therapeutic exposure; rather, it depends on both location and time. For this reason, the transport layer required for the coupled microbiome model is provided by the simulation.

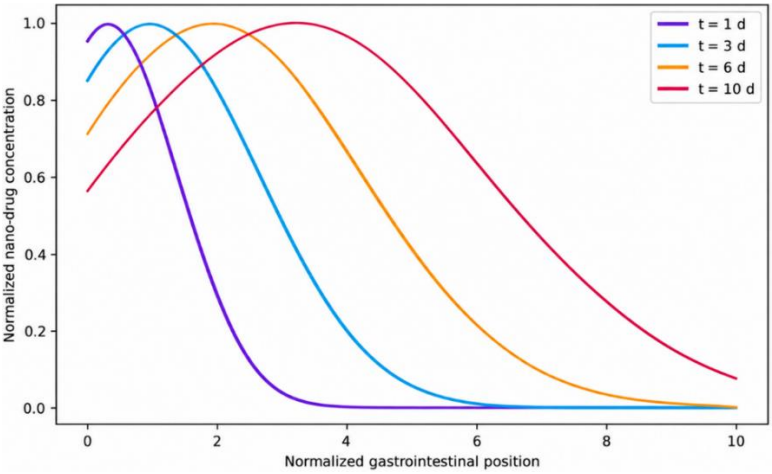


Figure 4: Concentration Profiles of Nano-drugs Showing Degradation, Advection, and Diffusion Over Time

5.5. Coupled Spatiotemporal Microbiome Response

Table 5 displays the chosen states from the spatiotemporal model for equal time steps. The data set is designed to show the temporal orderliness of the community's diversity, microbial biomass, and treatment exposure. The values could be used as references for recovery timings and the patterns shown.

Table 5: Numerical Values for Nano-Drug Transport for Coupled Spatiotemporal Microbiome Response

Time (day)	Biomass	Diversity	Drug exposure
0.0	0.900	0.840	0.100
4.0	0.620	0.730	0.780
8.0	0.510	0.680	0.520
12.0	0.580	0.710	0.340
16.0	0.700	0.770	0.220
20.0	0.790	0.810	0.140

Figure 5 shows that while normalized biomass initially and then recovered, diversity changed more gradually and eventually reached a limited regime after treatment. There was a noticeable lag between the forcing and the state because the medication dosage peaked before biomass recovery took over. The microbial state in this sequence is dependent on both the present and past exposure to ecological feedback, supporting a nonlinear dynamical system.

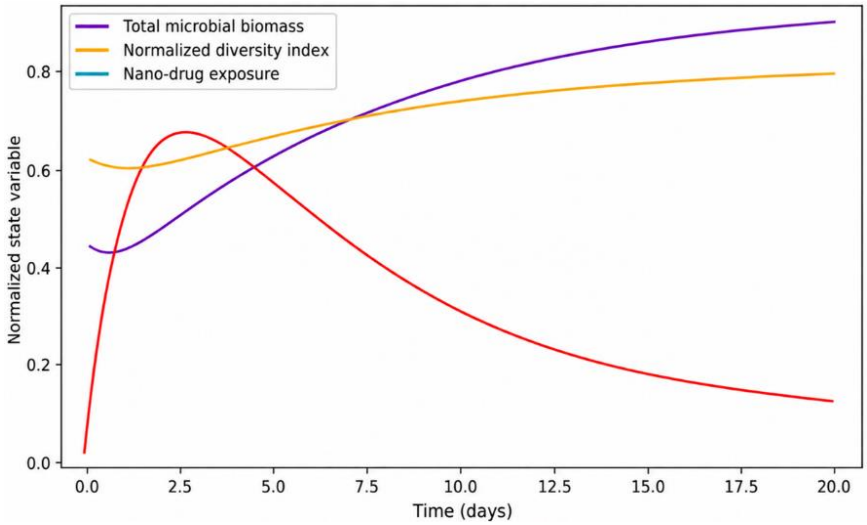


Figure 5: Microbe Biomass, Diversity, and Exposure to Nano-drugs

Trajectories exhibit limited behavior, suggesting the parameterization selected does not cause the population under consideration to either collapse or increase unstably. In terms of phase-space representation, the process begins with the system moving away from its starting location during treatment, and when the exposure level drops, it reaches a new attractor position. The biomass and diversity recovery processes do not

have to be simultaneous, as evidenced by the time disparity between them. Therefore, the suggested coupled model provides a way to assess recovery following therapy and explains ecological relaxation and transport kinetics.

5.6. Adaptive Network Topology and Treatment-Associated Analysis

Table 6 summarizes metrics related to network structure at different treatment intensity levels. Modularity is a measure of how easily nodes can be divided into clusters, where connections exist within clusters but not between them. Mean degree is the average number of connections that each node possesses.

Table 6: Network Topology Metrics Across Treatment Intensities

Treatment Intensity	Mean Degree	Modularity
0.0	5.8	0.34
0.1	5.672	0.36
0.2	5.526	0.379
0.3	5.35	0.397
0.4	5.136	0.415
0.5	4.89	0.433
0.6	4.621	0.449
0.7	4.347	0.465
0.8	4.086	0.481
0.9	3.853	0.496
1.0	3.656	0.51

In Figure 6, adaptive network analysis showed that when normalized treatment intensity increased, the mean degree systematically decreased and the modular structure increased in tandem. Increased modularity suggests that these connections are increasingly compartmentalized, and decreased mean degree suggests that there are fewer direct ecological interactions that are robustly retained at greater levels of treatment. A network may simultaneously get more-sparse and organized, which makes this mathematically significant. By establishing semi-independent modules, such reorganization can reduce the transmission of perturbations in the network. This entails examining the network of microbial nodes with weighted edges in connection to a treatment parameter that can be changed.

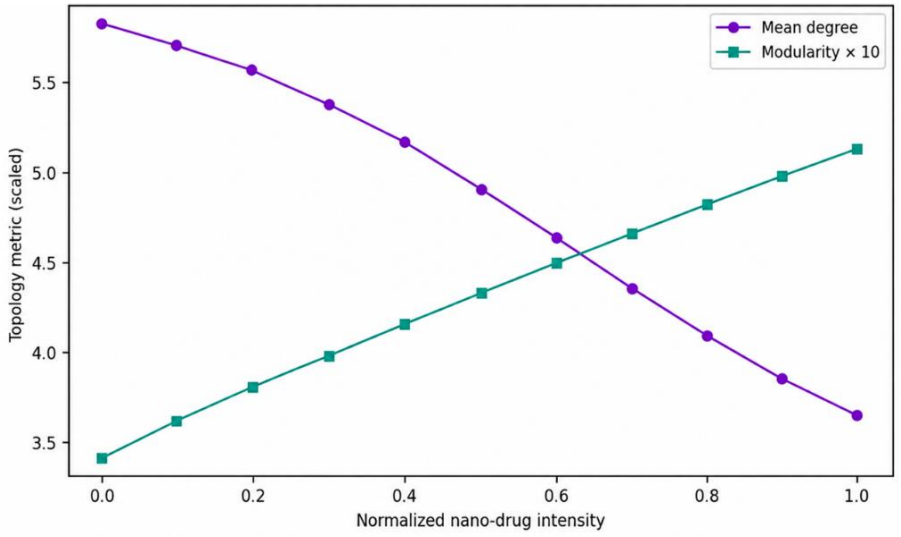


Figure 6: Mean Degree and Modularity Concerning the Normalized Intensity of Nano-drug Therapies

5.7. Stability, Global Sensitivity, Therapeutic Response and Integrated Recovery

Table 7 summarizes the numerical values for the four analytical methods displayed in Figure 7 (a–d). The migration parameter ρ is associated with the equilibrium stability score in stability analysis; the normalized treatment intensity is associated with the Therapeutic Response Index (TRI) in response analysis; the values are normalized global sensitivity measures of the principal parameters in sensitivity analysis; and the table displays the treatment's saturation response and favorable migration region in recovery analysis.

Table 7: Numerical findings for integrated recovery, sensitivity analysis, treatment effectiveness, and stability

Analysis	Parameter and condition	Representative output
Equilibrium stability	ρ =0.00	0.450
Equilibrium stability	ρ =0.10	0.451
Equilibrium stability	ρ =0.20	0.456
Equilibrium stability	ρ =0.30	0.479
Equilibrium stability	ρ =0.40	0.543
Equilibrium stability	ρ =0.50	0.671
Equilibrium stability	ρ =0.60	0.831
Equilibrium stability	ρ =0.65	0.894
Equilibrium stability	ρ =0.70	0.927
Equilibrium stability	ρ =0.75	0.923
Equilibrium stability	ρ =0.80	0.883
Equilibrium stability	ρ =0.90	0.736
Equilibrium stability	ρ =0.95	0.656
Equilibrium stability	ρ =1.00	0.587
Therapeutic response (TRI)	Normalized treatment intensity = 0.0	0.280
Therapeutic response (TRI)	Normalized treatment intensity = 0.5	0.761
Therapeutic response (TRI)	Normalized treatment intensity = 1.0	0.799
Global sensitivity	Growth rate	0.740
Global sensitivity	Carrying capacity	0.580
Global sensitivity	Drug efficacy	0.510
Global sensitivity	Drug diffusion	0.360
Global sensitivity	Interaction strength	0.310
Global sensitivity	Migration rate	0.240
Integrated recovery	Favorable migration region	$\rho \approx 0.70$
Integrated recovery	Treatment response	Increasing with saturation

The four modeling results that characterize the non-linear behavior of the proposed networked microbiome system are combined in Figure 7 (a–d). The non-monotonic stability response to migration allocation is shown in Figure 7(a), the stability index increases from the low migration regime, peaks at $\rho \approx 0.70$, and subsequently decreases. It indicates that rather than a general benefit of the increase in migration, there is a beneficial regime of redistribution. This control law is associated with a better collection of linear system eigenvalues and, hence, better local asymptotic stability. Figure 7(b) represents that when the strength of the therapeutic intervention is low to moderate, the Therapeutic Response Index increases rapidly before saturating. This implies a declining marginal response to a high-intensity intervention. Figure 7(c) illustrates the respective contributions of the three variables i.e. growth rate, carrying capacity, and therapeutic effectiveness to the sensitivity. In the given parameter configuration, diffusion, interactions, and migration contribute comparatively less to sensitivity. Figure 7(d) illustrates how therapy and migration work together to support the healing process.

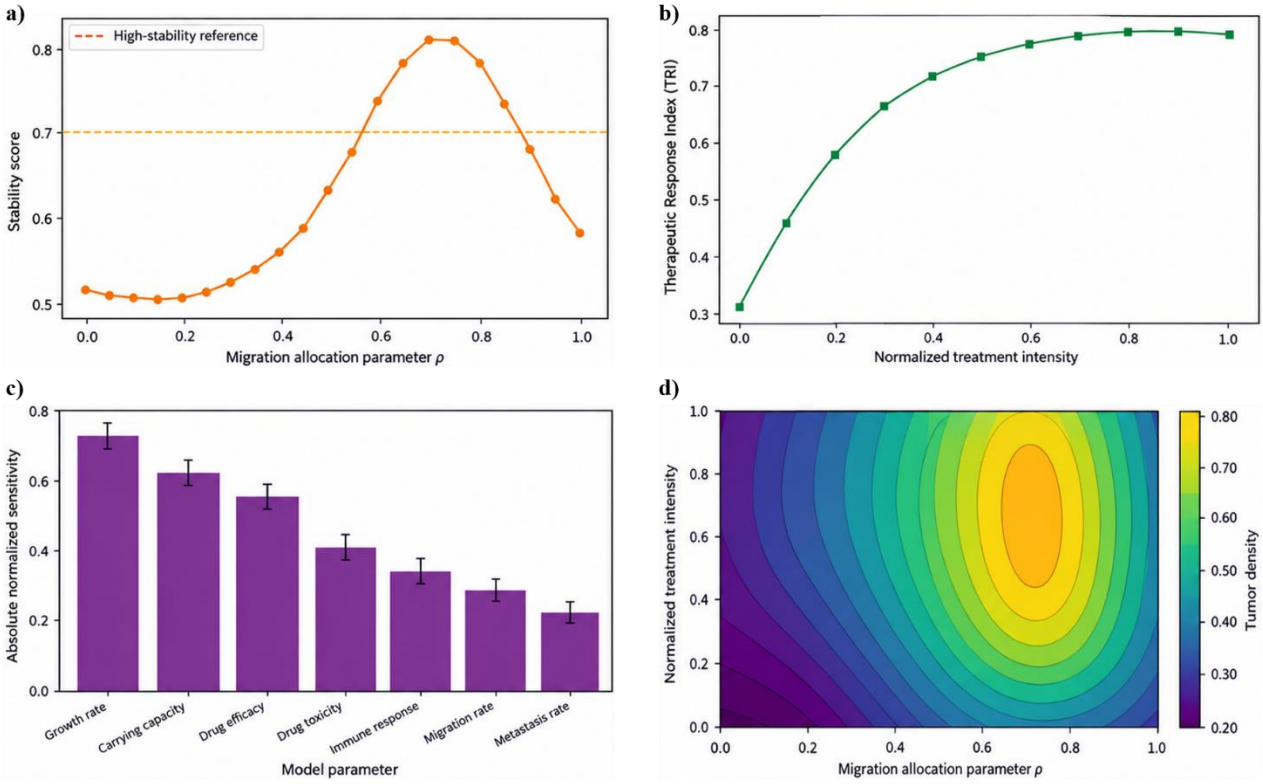


Figure 7: (a) Stability at Equilibrium in Connection with the Migration-Allocation Parameter ρ, (b) Therapeutic Response Index Regarding the Normalized Intensity of Treatment, (c) Normalized Global Sensitivity of the Primary Model Parameters, and (d) Combined Recovery Landscape Concerning Migration Allocation and Treatment Intensity

6. Discussion

The model's dynamics demonstrate that the therapeutic efficacy depends on the coupled effects of the microorganisms' growth rate, interaction strength, migration, and spatial availability rather than just the therapy's intensity. The existence of positive equilibria and damped oscillations suggests convergence to a suitable long-term state from the perspective of dynamical systems theory. The dissipation in non-linear dynamics is suggested by the damped oscillations and bounded positive equilibria; redistribution with delay resulting from finite movement across compartments is implied by the delayed reaction. Similarly, two patch streams and mobility impact microbial coexistence and stability, as shown by mathematically organized spatial models (Cao et al., 2022; Shibasaki & Mitri, 2023). This addition is made possible by the existing architecture, which allows the drug realm to continuously modify the microbiome's dynamics. The path dependency results from the states of each population being dependent on the local ecological conditions and the dynamic history of exposure. Thus, bounded trajectories should be seen as dynamical admissibility attractor regimes (Revel-Muroz et al., 2023).

A further mathematical explanation of treatment effects is provided by the results of the network analysis. The generalized Lotka-Volterra equation's equilibrium configuration and effective interaction matrix are thus altered by the impact of therapy on the interaction strength. The community reconfiguration process is complementarily described by the combination of network structure and dynamical stability. In addition to revealing microbial hubs at pertinent time scales, dynamic network analysis has demonstrated that the microbiome network structure is not static but rather varies based on the biological state (Li et al., 2023). Therefore, the generalized Lotka-Volterra dynamics and equilibrium structure may be affected by therapy-induced changes in the interaction strength. This research is made more rigorous by combining network topology, kinetics, and stability theory.

The transport data emphasize that in order to comprehend the effects of nano-drugs, a spatiotemporal exposure field is necessary. The combined effects of advection, diffusion, and degradation result in greater spreading, attenuation, and displacement of the concentration peak. As a result, the microbial population in the

gastrointestinal system will experience various stresses from the same nominal dosage. The significance of mucosa contact, gastrointestinal transit, nanotherapeutic targeting, and release is highlighted by recent studies (Chen et al., 2023; Lang et al., 2023; Peng et al., 2023). These processes are described by transport and release rates in the current framework, allowing their effects to be distinguished from those of the ecological factors. Additionally, coupled dynamics show that biomass and diversity recover at distinct timeframes, suggesting that their typical reaction periods range. Therefore, rather than just being an endpoint, recovery should be viewed as a trajectory in ecological state space. This knowledge aligns with multiscale spatial modeling, in which interactions and transit lead to the microorganisms' structure (Aminian-Dehkordi et al., 2025).

The stability, sensitivity, and TRI criteria are used to numerically differentiate treatment regimens. The system's maximum stability is provided by an intermediate migration-allocation regime, which suggests that the system's local dynamics are non-monotonously dependent on redistribution rather than being positively impacted by increasing migration. At an intermediate migration-allocation level, stability is at its peak. This indicates that there is an inner maximum point rather than a monotone benefit from more migrations. The TRI value's fast rise and subsequent saturation point to a declining marginal benefit at increasing treatment intensities. Diffusion, interaction, and migration are less important in terms of sensitivity than the drug's growth rate, carrying capacity, and effectiveness. This is consistent with ecological models showing that resilience in microbiomes may be defined using stability metrics and multiscale models showing how spatial structure and metabolism can result in emergent states (Qiao et al., 2024; Revel-Muroz et al., 2023). Furthermore, recent advancements in nanomaterials have demonstrated that the settings and composition of microorganisms influence their reactivity (Kumar et al., 2024). This paradigm may be used to monitor recovery, identify stability windows, and differentiate transport from ecology. However, the regime of trajectories is just theoretical at this time because it is modeled rather than collected from patients.

7. Conclusion

This study offers a mathematical model that describes the interaction between nano-drug and microbiome as a connected dynamic process rather than merely a concentration effect. Population dynamics, interspecies interaction, migration, exposure, deterioration, and therapy are all represented mathematically. This enables us to comprehend how both dynamical and network techniques can be used to characterize changes in the status of microbiome populations. The non-dimensional representation makes it possible to compare various processes at different scales and aids in determining the parameters governing the behavior of the system. Non-linear thresholds, heterogeneous spatial forcing, and parameter dependency on stability in treatment response are all revealed by this approach. Stability and sensitivity measures aid in determining which states are relatively stable or sensitive to perturbation within specific regimes, and descriptors of network topology incorporate information about structural dynamics into the dynamics of the population system through measurements of change in connectivity and structure. Another scalar representation of the multidimensional result is the treatment response index. In terms of methodology, the main contribution is the integration of the previously described components into a single prediction framework. Such a framework will be helpful in developing theories regarding the microbial community's resilience and in conducting methodical comparisons across various treatment situations. Such a framework could be expanded in the future to accommodate random disturbances, additional functional groups of microorganisms, empirical estimates of transport coefficients, and patient-specific parameter distribution.

8. References

Alzubadi, H. (2025). Dynamical analysis of microbiome-based tumor therapeutics using a fractional derivative approach. *International Journal of Biomathematics*, 2550145.

Aminian-Dehkordi, J., Dickson, A., Valiei, A., & Mofrad, M. R. (2025). Meta Biome: A multiscale model integrating agent-based and metabolic networks to reveal spatial regulation in gut mucosal microbial communities. *Msystems*, *10*(5), e01652-01624.

Cao, X., Dong, A., Kang, G., Wang, X., Duan, L., Hou, H., Zhao, T., Wu, S., Liu, X., & Huang, H. (2022). Modeling spatial interaction networks of the gut microbiota. *Gut Microbes*, *14*(1), 2106103.

Chen, C., Beloqui, A., & Xu, Y. (2023). Oral nanomedicine biointeractions in the gastrointestinal tract in health and disease. *Advanced drug delivery reviews*, *203*, 115117.

Culp, E. J., & Goodman, A. L. (2023). Cross-feeding in the gut microbiome: ecology and mechanisms. *Cell host & microbe*, *31*(4), 485-499.

Garbati, P., Picco, C., Magrassi, R., Signorello, P., Cacopardo, L., Dalla Serra, M., Faticato, M. G., De Luca, M., Balestra, F., & Scavo, M. P. (2024). Targeting the gut: a systematic review of specific drug nanocarriers. *Pharmaceutics*, *16*(3), 431.

Geng, J., Ji, B., Li, G., López-Isunza, F., & Nielsen, J. (2021). CODY enables quantitatively spatiotemporal predictions on in vivo gut microbial variability induced by diet intervention. *Proceedings of the National Academy of Sciences*, *118*(13), e2019336118.

Gonzalez-Garcia, J., Delgado-Villalobos, A., Hernandez-Ruiz, G., Díaz-Torres, O., García-Cayuela, T., Gradilla-Hernández, M. S., González-Avila, M., Gómez-Sandoval, J. R., Rodríguez-Montaño, R., & Bayardo-González, R. A. (2025). Synthetic microbial communities as novel models to study gut microbiome–host interactions in metabolic diseases. *Discover Endocrinology and Metabolism*, *1*(1), 12.

Gupta, Y., Sharma, B., & Jain, C. K. (2025). Advanced membrane simulations in probiotics and gut microbiome interaction research: the current trends and insights. *Current Pharmaceutical Design*.

Hadjigeorgiou, A. G., Harkos, C., Mishra, A. K., Morad, G., Johnson, S. B., Ajami, N. J., Wargo, J. A., Munn, L. L., Stylianopoulos, T., & Jain, R. K. (2025). Mathematical modeling and association analysis decipher the impact of the gut microbiome on cancer immunotherapy. *Cancer Research*, *85*(16), 3139-3155.

Irwin, C., Mignone, F., Montani, S., & Portinale, L. (2024). Graph neural networks for gut microbiome metaomic data: A preliminary work. *arXiv preprint arXiv:2407.00142*.

Kumar, A., Pramanik, J., Batta, K., Bamal, P., Gaur, M., Rustagi, S., Prajapati, B. G., & Bhattacharya, S. (2024). Impact of metallic nanoparticles on gut microbiota modulation in colorectal cancer: A review. *Cancer Innovation*, *3*(6), e150.

Lang, T., Zhu, R., Zhu, X., Yan, W., Li, Y., Zhai, Y., Wu, T., Huang, X., Yin, Q., & Li, Y. (2023). Combining gut microbiota modulation and chemotherapy by capecitabine-loaded prebiotic nanoparticle improves colorectal cancer therapy. *Nature communications*, *14*(1), 4746.

Lange, E., Kranert, L., Krüger, J., Benndorf, D., & Heyer, R. (2024). Microbiome modeling: a beginner's guide. *Frontiers in microbiology*, *15*, 1368377.

Lawing, A., & Bleich, R. (2025). Working together: gut microbe-microbe interactions shape host inflammation. *Infection and Immunity*, *93*(7), e00512-00524.

Li, X., Lu, X., Liu, M., Zhang, Y., Jiang, Y., Yang, X., & Man, C. (2024). The immunomodulatory effects of A2 β-casein on immunosuppressed mice by regulating immune responses and the gut microbiota. *Nutrients*, *16*(4), 519.

Li, Y., Chen, Y., Fan, Y., Chen, Y., & Chen, Y. (2023). Dynamic network modeling of gut microbiota during Alzheimer's disease progression in mice. *Gut Microbes*, *15*(1), 2172672.

Luo, M., Zhu, J., Jia, J., Zhang, H., & Zhao, J. (2024). Progress on network modeling and analysis of gut microecology: a review. *Applied and Environmental Microbiology*, *90*(3), e00092-00024.

Peng, P., Feng, T., Yang, X., Nie, C., Yu, L., Ding, R., Zhou, Q., Jiang, X., & Li, P. (2023). Gastrointestinal microenvironment responsive nanoencapsulation of probiotics and drugs for synergistic therapy of intestinal diseases. *ACS nano*, *17*(15), 14718-14730.

Qiao, X., Bao, L., Liu, G., & Cui, X. (2024). Nanomaterial journey in the gut: from intestinal mucosal interaction to systemic transport. *Nanoscale*, *16*(41), 19207-19220.

Revel-Muroz, A., Akulinin, M., Shilova, P., Tyakht, A., & Klimenko, N. (2023). Stability of human gut microbiome: Comparison of ecological modelling and observational approaches.

Sego, T., Aponte-Serrano, J. O., Ferrari Gianlupi, J., Heaps, S. R., Breithaupt, K., Brusch, L., Crawshaw, J., Osborne, J. M., Quardokus, E. M., & Plemper, R. K. (2020). A modular framework for multiscale, multicellular, spatiotemporal modeling of acute primary viral infection and immune response in epithelial tissues and its application to drug therapy timing and effectiveness. *PLoS computational biology*, *16*(12), e1008451.

Shibasaki, S., & Mitri, S. (2023). A spatially structured mathematical model of the gut microbiome reveals factors that increase community stability. *Iscience*, *26*(9).

Sieders, M., Candry, P., & El Aidy, S. (2025). Hydrogel-based experimental models of the gastrointestinal tract. *Microbiome*, *13*(1), 1-27.

Simonson, M., Simonson, T., & Nobécourt, E. (2025). An overview of basic pathophysiological interactions between gut bacteria and their host. *Frontiers in nutrition*, *12*, 1565609.

Urtecho, G., Moody, T., Huang, Y., Sheth, R. U., Richardson, M., Descamps, H. C., Kaufman, A., Lekan, O., Zhang, Z., & Velez-Cortes, F. (2024). Spatiotemporal dynamics during niche remodeling by super-colonizing microbiota in the mammalian gut. *Cell systems*, *15*(11), 1002-1017. e1004.

Zhang, M., Ma, W., Zhang, J., He, Y., & Wang, J. (2018). Analysis of gut microbiota profiles and microbe-disease associations in children with autism spectrum disorders in China. *Scientific Reports*, *8*(1), 13981.